Utah Uranium General

Mineralium Deposita (1998) 33: 477–494

ARTICLE

C. G. Cunningham · J. D. Rasmussen · T. A. Steven
R. O. Rye · P. D. Rowley
S. B. Romberger · J. Selverstone

Hydrothermal uranium deposits containing molybdenum and fluorite in the Marysvale volcanic field, west-central Utah

Received: 23 June 1997 / Accepted: 15 October 1997

Abstract Uranium deposits containing molybdenum and fluorite occur in the Central Mining Area, near Marysvale, Utah, and formed in an epithermal vein system that is part of a volcanic/hypabyssal complex. They represent a known, but uncommon, type of deposit; relative to other commonly described volcanic-related uranium deposits, they are young, well-exposed and well-documented. Hydrothermal uranium-bearing quartz and fluorite veins are exposed over a 300 m vertical range in the mines. Molybdenum, as jordisite (amorphous MoS_2), together with fluorite and pyrite, increase with depth, and uranium decreases with depth. The veins cut 23-Ma quartz monzonite, 20-Ma granite, and 19-Ma rhyolite ash-flow tuff. The veins formed at 19-18 Ma in a 1 km^2 area, above a cupola of a composite, recurrent, magma chamber at least 24 × 5 km across that fed a sequence of 21- to 14-Ma hypabyssal granitic stocks, rhyolite lava flows, ash-flow tuffs, and volcanic domes. Formation of the Central Mining Area began when the intrusion of a rhyolite stock, and related molybdenite-bearing, uranium-rich, glassy rhyolite dikes, lifted the fractured roof above the stock. A breccia pipe formed and relieved magmatic pressures, and as blocks of the fractured roof began to settle back in place, flat-lying, concave-downward, "pull-apart" fractures were formed. Uranium-bearing, quartz and fluorite veins were deposited by a shallow hydrothermal system in the disarticulated carapace. The veins, which filled open spaces along the high-angle fault zones and flat-lying fractures, were deposited within 115 m of the ground surface above the concealed rhyolite stock. Hydrothermal fluids with temperatures near 200 °C, $\delta^{18}O_{H_2O} \sim -1.5$, $\delta D_{H_2O} \sim -130$, log fO_2 about −47 to −50, and pH about 6 to 7, permeated the fractured rocks; these fluids were rich in fluorine, molybdenum, potassium, and hydrogen sulfide, and contained uranium as fluoride complexes. The hydrothermal fluids reacted with the wallrock resulting in precipitation of uranium minerals. At the deepest exposed levels, wallrocks were altered to sericite; and uraninite, coffinite, jordisite, fluorite, molybdenite, quartz, and pyrite were deposited in the veins. The fluids were progressively oxidized and cooled at higher levels in the system by boiling and degassing; iron-bearing minerals in wall rocks were oxidized to hematite, and quartz, fluorite, minor siderite, and uraninite were deposited in the veins. Near the ground surface, the fluids were acidified by condensation of volatiles and oxidation of hydrogen sulfide in near-surface, steam-heated, ground waters; wall rocks were altered to kaolinite, and quartz, fluorite, and uraninite were deposited in veins. Secondary uranium minerals, hematite, and gypsum formed during supergene alteration later in the Cenozoic when the upper part of the mineralized system was exposed by erosion.

Editorial handling: R. Goldfarb

C.G. Cunningham (✉)
US Geological Survey, 954 National Center,
Reston, Virginia 20192
e-mail: cunningham@usgs.gov Fax: (703) 860-6383

J.D. Rasmussen
North American Exploration, 497 N. Main Street,
Kaysville, Utah 84037

T.A. Steven
US Geological Survey, MS 913, Box 25046,
Denver Federal Center, Denver, Colorado 80225

R.O. Rye
US Geological Survey, MS 963, Box 25046,
Denver Federal Center, Denver, Colorado 80225

P.D. Rowley
US Geological Survey, 6770 South Paradice Road,
Las Vegas, NV 89119

S.B. Romberger
Department of Geology and Geological Engineering,
Colorado School of Mines, 1516 Illinois Street,
Golden, Colorado 80401-1887

J. Selverstone
Department of Earth and Planetary Sciences,
Northrop Hall Room 141, University of New Mexico,
200 Yale Boulevard, NE, Albuquerque,
New Mexico 87131-1116

Introduction

The most productive uranium deposits in the Marysvale volcanic field of west-central Utah are in the Central Mining Area (Fig. 1). These uranium deposits contain significant quantities of fluorite and molybdenum. The deposits consist of hydrothermal quartz and fluorite veins that cut granitic and volcanic rocks and are interpreted to have formed in an epithermal vein system that is part of a volcanic/hypabyssal complex. They represent a known, but uncommon, type of deposit. Other deposits having some similar features include Jamestown, Colorado (Goddard 1935, 1946; Phair and Shimamoto 1952; Kelly and Goddard 1969; Nash and Cunningham 1973), Rexpar, Southern British Columbia (Preto 1978; Morton et al. 1978; Curtis 1981), Maureen, Northeast Queensland, Australia (O'Rourke 1975), Spor Mountain, Thomas Range, Utah (Staatz and Osterwald 1956, 1959; Lindsey 1981); and Sierra de Peña Blanca, Chihuahua, Mexico (Goodell 1985; George-Aniel et al. 1985). Relative to many of the other volcanic-related uranium deposits described here, the Central Mining Area deposits are young, well-exposed, and well-documented. Uranium was discovered there in 1949 and at least 6.4×10^5 kg of U_3O_8 were produced by 1962 (Bromfield et al. 1982). Since then, only sporadic exploration and development work has been undertaken and the mines are presently closed. The grade of ore at Marysvale was typically a few tenths of a percent uranium (Walker and Osterwald 1963). The known vertical occurrence of uranium-bearing minerals, according to mine workings and drill hole data, is at least 600 m (Taylor et al. 1951).

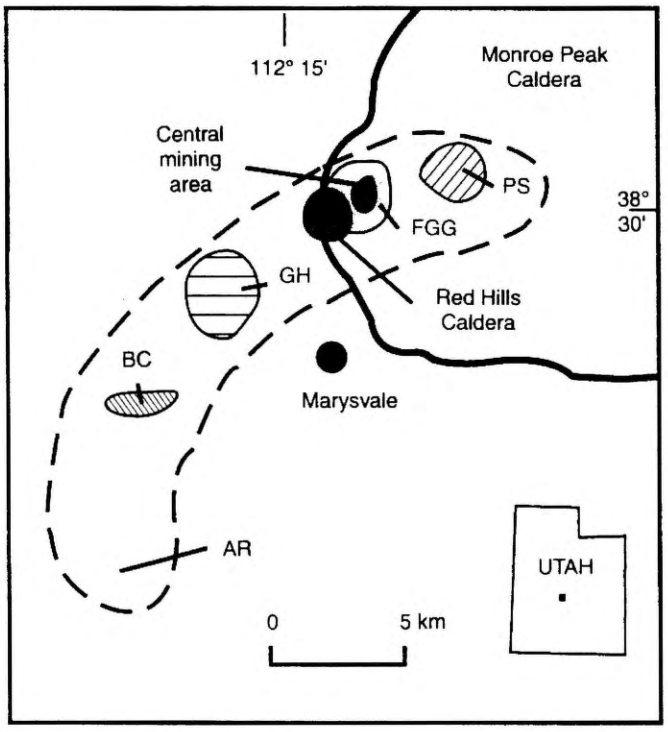

Fig. 1 Location map of igneous rocks, volcanic features, and the Central Mining Area in the eastern source area of the Mount Belknap Volcanics. This shows 23 Ma *Monroe Peak caldera*; PS, 21 Ma porphyritic stocks and volcanic domes; *FGG*, 20 Ma fine-grained granite; *Red Hills Caldera*, source of 19 Ma Red Hills Tuff; *GH*, 18 Ma Gray Hills Rhyolite Member; *BC*, 16 Ma Beaver Creek stock; *AR*, 14 Ma Alunite Ridge includes Alunite Ridge center and Deer Trail Mountain center

The Central Mining Area is located about 260 km south of Salt Lake City and 5.6 km north-northeast of the town of Marysvale in the central part of the Marysvale volcanic field. Callaghan (1939) published the first comprehensive study of the igneous rocks in the area. Paul Kerr and his students P.M. Bethke, G.P. Brophy, H.M. Dahl, J. Green, L.E. Woodward, and N.W. Molloy, of Columbia University, under the auspices of the US Atomic Energy Commission, prepared many reports on the area, which are summarized in Kerr et al. (1957) and Kerr (1968). Other pertinent publications include Gruner et al. (1951), Walker and Osterwald (1956), Gilbert (1957), Callaghan and Parker (1961), Willard and Callaghan (1962), Callaghan (1973), and Shea and Foland (1986). The US Geological Survey (USGS) began a study of the volcanic geology and ore deposits of the area in the mid-1970s that has continued to the present. The volcanic setting and geochronology, and descriptions of other deposits in the volcanic field, are in Cunningham and Steven (1979a); Steven et al. (1979, 1984); Steven and Morris (1987) and Rowley et al. (1988a, b, 1994). Brief overviews of the tectonic setting are in Cunningham et al. (1994, 1997). Cunningham and Steven (1979b) suggested that the uranium vein system of the Central Mining Area may be underlain by a climax-type porphyry molybdenum deposit; that suggestion is still valid but is as yet untested. Brief, descriptive overviews, and abstracts that include the uranium deposits, are Steven et al. (1981); Cunningham et al. (1980) and Rasmussen et al. (1985). This study presents a genetic model of the deposits. Relevant major publications on uranium veins in volcanic rocks include US Geological Survey (1963), Rich et al. (1977), Goodell and Waters (1981), and the International Atomic Energy Agency (1985).

Geologic setting

The Marysvale volcanic field is one of the largest volcanic fields in the western United States and is located in the High Plateaus subprovince between the Colorado Plateau and the Basin and Range Provinces. The field consists of middle to upper Tertiary volcanic rocks which unconformably overlie Mesozoic and lower Cenozoic sedimentary rocks. Most of the volcanic rocks in the field are part of an intermediate-composition, calc-alkaline sequence that was erupted from about 35 to 22 Ma. The Central Mining Area lies at the western margin of the 23-Ma Monroe Peak caldera, the largest caldera in the Marysvale volcanic field (Steven et al. 1984; Rowley et al. 1988a,b). A principle host for the uranium ore deposits described here is a quartz monzonite porphyry called the Central Intrusion (formerly called the "Central intrusive" by Kerr et al. 1957) which is a late stock associated with the Monroe Peak

caldera. The Central Intrusion is surrounded by 23 Ma replacement alunite deposits (Cunningham et al. 1984) that are underlain by pyrite-bearing, propylitically altered volcanic rocks.

Volcanic rock compositions changed abruptly at about 22 Ma, and a bimodal sequence of alkali rhyolite and basalt lava flows and associated igneous rocks were erupted from 22-14 Ma. Regional extension near Marysvale was generally associated with the bimodal volcanism (Anderson and Rowley 1975; Steven et al. 1979; Best et al. 1980; Rowley et al. 1988a). The change from intermediate to bimodal volcanism at about 22 Ma is interpreted as reflecting the change from subduction to transform motion along the western margin of the United States (Cunningham et al. 1994, 1997; Rowley et al. 1994). The alkali rhyolite rocks, called the Mount Belknap Volcanics (Steven et al. 1979), are a series of volcanic domes, lava flows, and ash-flow tuffs that were erupted from two source areas. The western source area is in the central Tushar Mountains and is manifested mainly by the 19-Ma Mount Belknap caldera (Cunningham and Steven, 1979a; Steven et al. 1979, 1981; Budding et al. 1987). The eastern source area is an elongate area about 24 km long and 5 km wide that extends from northeast of Marysvale, southwestward to Alunite Ridge/Deer Trail Mountain (Figs. 1 and 2). Igneous activity progressed from northeast toward the southwest, and with time, changed systematically in location, bulk composition, and phenocryst and volatile content. Volcanic activity began at 21 Ma with the extrusion of porphyritic volcanic domes and associated stocks (PS in Fig. 1), 8 km northeast of Marysvale. A hypabyssal, fine-grained granite stock (FGG in Fig. 1) was intruded at 20 Ma; it underlies much of the Central Mining Area and is one of the hosts of the uranium deposits. The focus of igneous activity moved slightly to the southwest with the eruption of a volatile-rich, alkali rhyolite tuff (the Red Hills Tuff Member of the Mount Belknap Volcanics) at 19 Ma and the Red Hills caldera subsided in response. Hydrothermal uranium mineralization, spatially and genetically related to glassy dikes that cut the Red Hills Tuff, took place at 19-18 Ma (Cunningham et al. 1982). Igneous activity continued to progress towards the southwest with the eruption of volatile-rich alkali rhyolite lavas (the Gray Hills Rhyolite Member of the Mount Belknap Volcanics; GH in Fig. 1) at 18 Ma and the intrusion of the small, Beaver Creek stock (unit BC in Fig. 1) and a rhyolite dike at the nearby Copper Belt mine at 16 Ma. The last major episode associated with the Mount Belknap Volcanics was at the southwestern end of the eastern source area (Figs. 1 and 2) at 14 Ma with the formation of gold, silver, base-metal mantos at Deer Trail Mountain and alunite deposits at Alunite Ridge. These deposits have been interpreted to be genetically related to two cupolas on an unexposed stock, one cupola beneath Alunite Ridge and the other under the summit of Deer Trail Mountain (Cunningham and Steven 1979c; Cunningham et al. 1984; Beaty et al. 1986; Rye 1993; Cunningham et al. 1996).

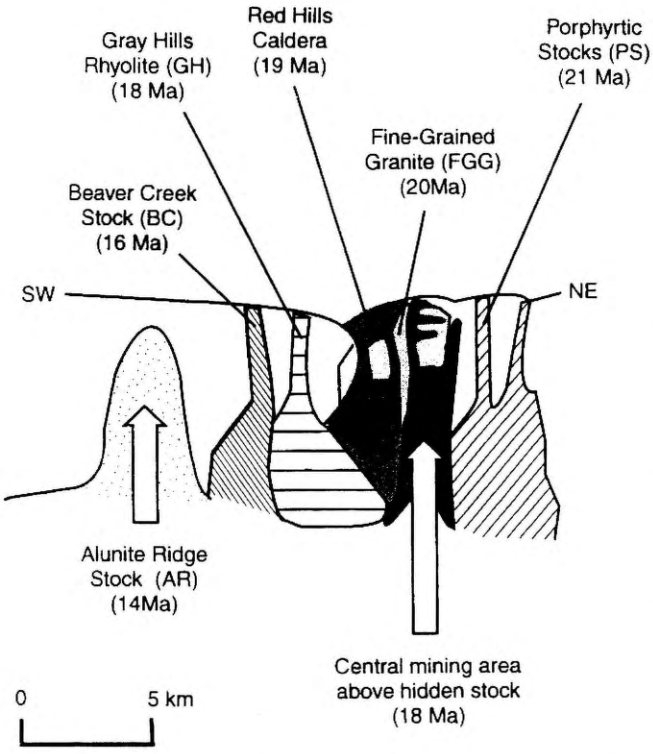

Fig. 2 Diagrammatic sketch showing postulated relations in the roots of source areas for the Mount Belknap Volcanics. Same units as Fig. 1

Central Mining Area

The Central Mining Area was mined almost exclusively for uranium and most of the uranium production has been from nine mines (Prospector, Freedom No. 1 and No. 2, Bullion Monarch, Farmer John, Cloys, Potts, Wilhelm, and Sunnyside) in an oval area about 1 km by 0.5 km across (Callaghan 1973). Base-metal sulfide minerals are essentially absent at Marysvale; however, molybdenum and fluorite are relatively abundant and a trace of gold has been reported.

The most recently published 1:24 000 scale geologic maps in the area are by Rowley et al. (1988a,b) who show that the Central Mining Area is located within the western boundary of the Monroe Peak caldera. The detailed geologic map, cross sections, and mine workings of the area (Fig. 3A–D) were constructed from surface and underground mapping done when the mines were open during exploration. Figure 3B (cross section A-A′ of Fig. 3A) approximately follows a > 500-m-long cross-cut that connects the 300 level on the Prospector mine on the south with the 700 level of the Freedom mines to the north. Table 1 contains descriptions and locations of samples analyzed for this report and Table 2 contains chemical analyses of the rocks.

Geology

Five significant rock types are shown on the geologic map and cross sections of the Central Mining Area (Fig. 3). The oldest is the 23-Ma Central Intrusion monzonite (Tci) that underlies much of the area. Dunkhase (1980) reported that the intrusion contains anomalously high contents of uranium, thorium, and zirconium. The Central Intrusion was intruded by the 20-Ma fine-grained granite (Tmf) which crops out just north of the mapped area and widens downward in the deeper levels of the mines of the Central Mining Area. The next unit, the 19-Ma alkali rhyolite Red Hills Tuff, caps a prominent north-trending ridge in the northeastern part on the mapped area (Fig. 3), where it unconformably overlies the Central Intrusion. The source of the Red Hills Tuff is the Red Hills caldera just west of the Central Mining Area. All of the aforementioned units are cut by brown, flow-banded, rhyolite dikes that are well

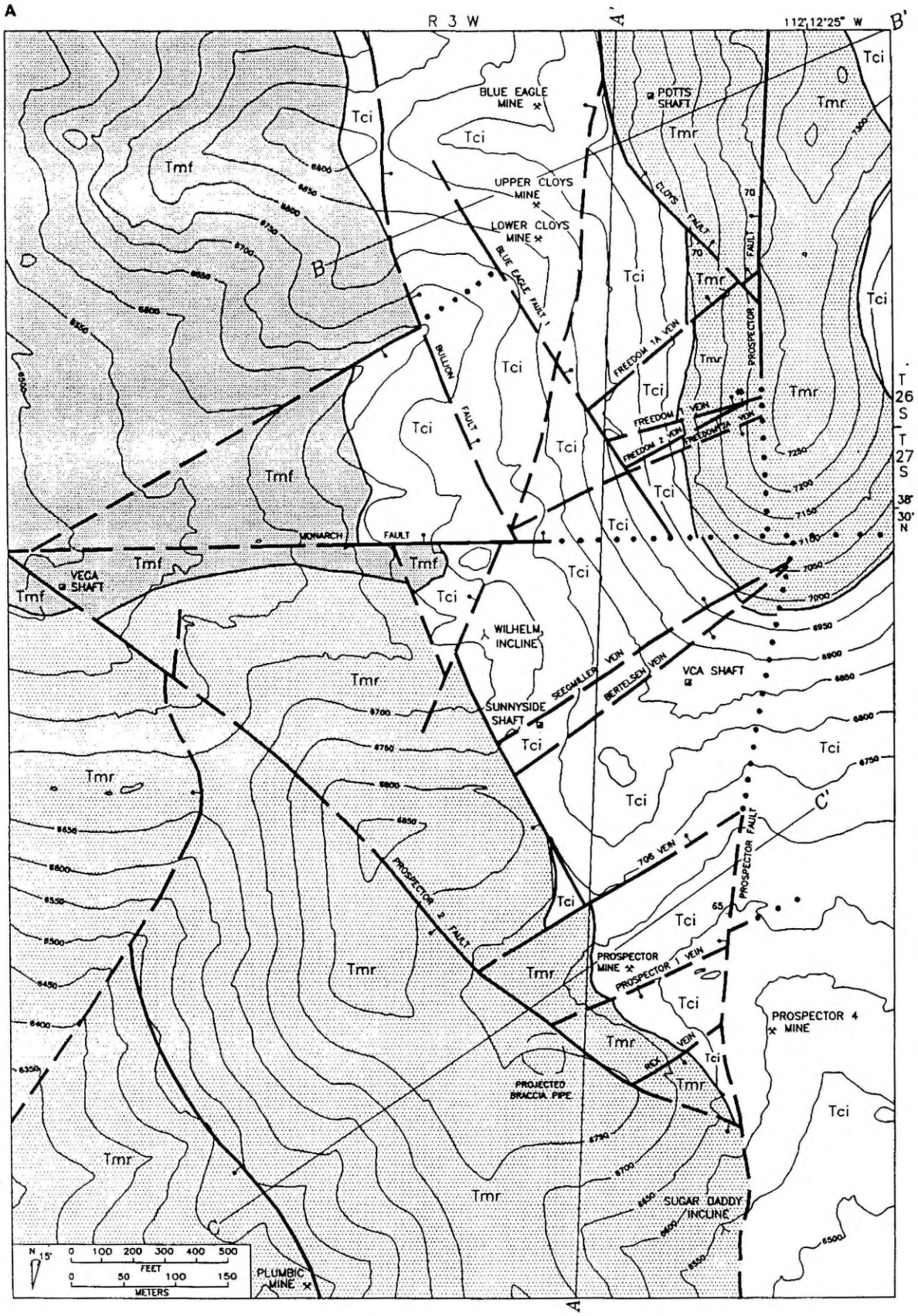
A
R 3 W
A'
112°12'25" W
B'
BLUE EAGLE MINE
POTTS SHAFT
UPPER CLOYS MINE
LOWER CLOYS MINE
CLOYS FAULT
BLUE EAGLE FAULT
BULLION FAULT
FREEDOM 1A VEIN
PROSPECTOR FAULT
FREEDOM VEIN
FREEDOM 2 VEIN
FREEDOM 3 VEIN
T 26 S
T 27 S
38° 30' N
MONARCH FAULT
VEGA SHAFT
WILHELM INCLINE
SEEGMILLER VEIN
BERTELSEN VEIN
VCA SHAFT
SUNNYSIDE SHAFT
706 VEIN
PROSPECTOR 2 FAULT
PROSPECTOR MINE
PROSPECTOR 1 VEIN
PROSPECTOR 4 MINE
PROJECTED BRACCIA PIPE
SUGAR DADDY INCLINE
PLUMBIC MINE
C'
C
B
D
Tmf
Tmr
Tci
N 15°
0 100 200 300 400 500 FEET
0 50 100 150 METERS

Fig. 3A

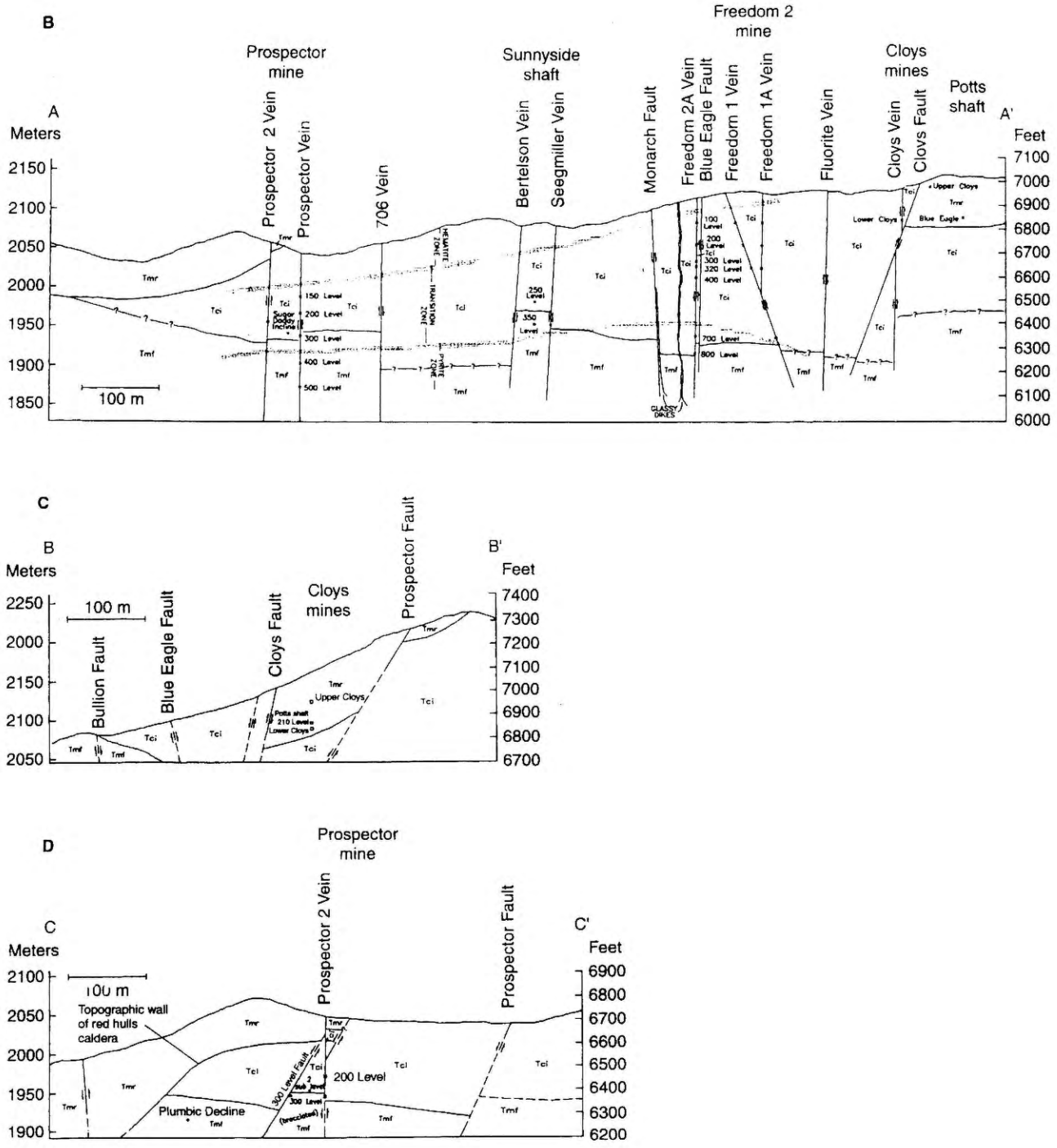

Fig. 3 **A** Geologic map and **B–D** cross sections of the Central Mining Area, Marysvale, Utah. *Tci*, 23-Ma porphyritic quartz monzonite (Central Intrusion); *Tmf*, 20-Ma fine-grained granite; *Tmr*, 19-Ma Red Hills Tuff Member of the Mount Belknap Volcanics; *glassy dikes*, 18-Ma glassy rhyolite dike. *Faults dashed* where uncertain, *dotted* where concealed; *bar and ball* on downthrown side. *Mine locations* projected into the plane of the cross section

exposed just east of the mapped area (sample M689) and underground in mine workings (see "Kerr's dike", Fig. 4; sample M408), on the Freedom 700 level cross-cut close to the VCA shaft (Fig. 3A)). Mineral separations of the glassy dikes contain minor biotite, hornblende, sphene, and molybdenite. The glassy dikes and uranium deposits have similar spatial distributions. The last significant rock type is a breccia that is composed of rounded to subangular fragments of the Central Intrusion in a matrix of comminuted rock and glassy rhyolite and, based on drilling, forms a vertical pipe. The breccia is exposed underground between the Sugar Daddy decline and the Prospector mine, but the area where it would project to the surface is covered by colluvium.

The uranium deposits have been dated at 19-18 Ma (Cunningham et al. 1982). A $^{207}Pb/^{204}Pb$-$^{235}U/^{204}Pb$ isochron age of 19.0 ± 3.7 Ma was obtained for

Table 1 Descriptions and locations of analyzed samples from the Central Mining Area, Marysvale, Utah

M29B	Colorless fluorite vein samples VCA-Freedom mine dump
M49A	Porphyritic, alkali rhyolite dome
M50	Fresh fine-grained granite, near the northern end of the Marysvale uranium district
M93	Red Hills Tuff, US highway 89 at Deer Creek
M270	Purple and clear fluorite veins cutting silicified quartz monzonite. Prospector mine dump
M403	Vein of euhedral quartz crystals with younger fluorite Deepest exposure of the 2 vein, Prospector mine, 300 level
M407	Fluorite-quartz vein, end of drift under Sunnyside shaft
M408A	Glassy rhyolite dike, ("Kerr's dike"). It is vertical and cuts quartz monzonite on the crosscut between the Prospector and Freedom mines. Zircon fission-track age of 18.1 ± 0.8 Ma and apatite age of 23.3 ± 4.7 Ma (Cunningham et al. 1982)
M444	Veins of euhedral quartz crystals cut by veins of purple fluorite Freedom 2 mine dump
M547B	Fluorite-quartz vein that cuts quartz monzonite. Same location as M701, M702, and M729. Vertical 2A vein on the Freedom 800 level
M600	Pyrite-bearing, sericite-bearing, fine-grained granite with miarolitic cavities, some lined by purple fluorite Plumbic mine dump. Sericite age of 21.1 ± 0.6 Ma (Cunningham et al. 1982)
M602	Pyrite-bearing uranium vein, Rex vein, prospector 4 mine, 12 m from 2 zone
M621	Fresh quartz monzonite, just west of Flattop hill
M663	Purple fluorite vein, sample from portal of the fluorite vein on west side of district
M667	Pyrite-fluorite-uranium veins in sample from dump of the Freedom mine
M674	Altered, punky, quartz monzonite with pervasive hematite, cut by sooty uranium veins. M674A is the red wall rock. Prospector 4 mine
M688	Relatively fresh, hard, quartz monzonite of the transition zone, cut by 1-cm-wide uranium vein that is bordered by 1-cm-wide band of hematite. Sample M688A is within the hematite zone. Sample M688B is outside the hematite zone, 5–9 cm from the vein
M689	Glassy rhyolite dike. Cuts quartz monzonite 1 km northeast of the Freedom mine. Zircon fission-track age is 19.0 ± 1.0 Ma (Cunningham et al. 1982)
M699	Pyrite-jordisite veins cutting fine-grained granite, Prospector mine, 300 level
M701	Uranium-purple/clear fluorite-quartz veins cutting fine-grained granite, same location as samples M702 and M729A. 2A vein, Freedom 800 level
M702	Fine-grained granite containing pyrite and cut by uranium-molybdenum veins, same location as samples M701 and M729A. 2A vein, Freedom 800 level
M704	Fine-grained granite adjacent to the 2a vein on the Freedom 900 level. Sample M704A is bleached and altered, within 5 cm of the vein, and gives a sericite age of 20.5 ± 0.7 Ma (Cunningham et al. 1982). Sample M704B is fresher than M704A, 5–10 cm from the vein
M706A	Altered quartz monzonite containing sooty uranium veins and some hematite
M711A	Altered, limonite-stained, quartz monzonite adjacent to Seegmiller vein, contains pyrite. Freedom 700 (Prospector 300) level
M714	Gray breccia containing angular fragments of quartz monzonite as much as several cm diameter in a gray matrix of rock flour and rhyolite glass. Sugar Daddy incline, 2 sublevel
M715A	Altered quartz monzonite, center of Seegmiller vein, by VCA headframe
M715B	Altered quartz monzonite, 10 cm from center of Seegmiller vein
M715C	Altered quartz monzonite, 25 cm from center of Seegmiller vein
M715D	Altered quartz monzonite, 36 cm from center of Seegmiller vein
M715E	Altered quartz monzonite, 51 cm from center of Seegmiller vein
M715F	Altered quartz monzonite, 183 cm from center of Seegmiller vein
M729	Purple fluorite-quartz-uranium veins containing jordisite and ilsemannite. Sample M729A is altered fine-grained granite adjacent to veins. Same location as M547, M701, and M702. 2A vein, Freedom 800 level
M766A	Altered, limonite-stained, quartz monzonite adjacent to high-grade uranium vein. Freedom 2 mine, depth unknown. Collected by Gerry Brophy
M767	Fluorite veins. Sample M767A is green fluorite and M767B is purple fluorite. Freedom mine, 1 vein, 1 upper level, about 30 m below present ground surface
M768	Green, purple, and clear fluorite veins. Sample M768A is green fluorite that appears younger than M768B (purple). 1A vein on the 1 upper level of the Freedom, about 30 m below present ground surface
M770	Purple fluorite-quartz-uranium veins containing jordisite and ilsemannite. Sample M770A is purple, M770C is clear, and M770D is purple fluorite. Same location as M729A. 2A vein, Freedom 800 level
M776	Pyrite-bearing quartz monzonite cut by fluorite veinlets. Drill site near south end of uranium mining district, sample is of drill core from the 267 m–284 m interval
M777	Pyrite-bearing, slightly-altered, fine-grained granite from dump of the Poison shaft. Mine workings do not extend far from the shaft
M793	Pyrite-bearing, fine-grained granite. Drill cuttings from hole LS 14-1, 116 m–128 m interval
M794	Pyrite-bearing fine-grained granite cut by uranium-fluorite bearing- Prospector 1 vein. Prospector mine, 500 level, west end of drift
M846	Pyrite-bearing fine-grained granite. Drill hole P4-4C, depth 268 m

Table 2 Analyses of Igneous rocks in the Marysvale Uranium District, Utah. Major oxides, and recalculated analyses on water-free basis, are in weight percent. U and Th in ppm

Field No. Ident.	M715A Altered Tci	M715B Altered Tci	M715C Altered Tci	M715D Altered Tci	M715E Altered Tci	M715F Altered Tci	M688A Hematite Tci	M688B Fresher Tci	M49A Porph dome	M704A Alt Tmf	M704B Alt Tmf	M50 Fresh Tmf	M502 Red Hills Tmr	M408A Kerr's dike
SiO_2	57.30	57.50	56.20	55.60	56.60	58.20	59.50	55.80	71.70	53.70	67.40	68.40	72.60	69.60
Al_2O_3	18.00	17.00	16.80	16.50	16.80	17.30	16.40	16.10	13.20	19.30	13.10	13.90	12.40	11.90
Fe_2O_3	3.71	5.08	6.78	6.30	4.80	4.96	2.54	2.37	1.10	4.23	3.34	1.15	0.72	0.55
FeO	0.38	0.32	0.45	0.88	1.89	1.35	2.64	3.21	0.44	0.59	0.62	1.07	0.24	0.24
MgO	1.10	1.10	1.30	1.70	1.90	1.40	2.20	1.80	0.45	1.20	0.97	0.86	0.23	0.27
CaO	2.09	1.83	2.19	2.05	3.42	3.05	2.10	5.36	1.10	1.26	0.54	1.58	0.55	2.00
Na_2O	2.30	2.20	2.50	2.30	3.20	3.30	2.90	3.00	3.70	0.20	1.00	2.10	3.70	1.80
K_2O	4.90	5.32	5.01	5.00	4.70	4.91	5.71	4.91	4.20	11.60	7.12	6.12	4.80	4.10
TiO_2	1.37	1.28	1.26	1.24	1.30	1.24	1.13	1.16	0.22	0.81	0.63	0.34	0.14	0.13
P_2O_5	0.56	0.50	0.50	0.50	0.59	0.50	0.40	0.40	0.14	0.30	0.20	0.10	0.03	0.01
MnO	0.02	0.02	0.19	0.04	0.10	0.12	0.08	0.10	0.05	0.22	0.05	0.05	0.06	0.07
H_2O+	2.58	2.39	2.32	2.09	0.98	1.01	1.49	0.86	2.60	1.75	1.26	1.25	3.40	5.40
H_2O	3.15	3.18	2.83	3.12	1.02	0.99	0.84	0.50	0.38	0.56	0.55	0.63	0.55	3.10
CO_2	0.01	0.01	0.02	0.01	0.01	0.02	0.74	2.50	0.02	0.91	0.15	0.99	0.02	0.03
TOTAL	97.47	97.73	98.35	97.33	97.31	98.35	98.67	98.07	99.30	96.63	96.93	98.54	99.44	99.20
SiO_2	62.47	62.40	60.31	60.36	59.39	60.42	62.24	59.23	74.45	57.49	70.97	71.50	73.01	76.76
Al_2O_3	19.62	18.45	18.03	17.91	17.63	17.96	17.15	17.09	13.71	20.66	13.79	14.53	12.47	13.12
Fe_2O_3	4.04	5.51	7.28	6.84	5.04	5.15	2.66	2.52	1.14	4.53	3.52	1.20	0.72	0.61
FeO	0.41	0.35	0.48	0.96	1.98	1.40	2.76	3.41	0.46	0.63	0.65	1.12	0.24	0.26
MgO	1.20	1.19	1.40	1.85	1.99	1.45	2.30	1.91	0.47	1.28	1.02	0.90	0.23	0.30
CaO	2.28	1.99	2.35	2.23	3.59	3.17	2.20	5.69	1.14	1.35	0.57	1.65	0.55	2.21
Na_2O	2.51	2.39	2.68	2.50	3.36	3.43	3.03	3.18	3.84	0.21	1.05	2.20	3.72	1.99
K_2O	5.34	5.77	5.38	5.43	4.93	5.10	5.97	5.21	4.36	12.42	7.50	6.40	4.82	4.52
TiO_2	1.49	1.39	1.35	1.35	1.36	1.29	1.18	1.23	0.23	0.87	0.66	0.36	0.14	0.14
P_2O_5	0.61	0.54	0.54	0.54	0.62	0.52	0.42	0.42	0.15	0.32	0.21	0.10	0.03	0.01
MnO	0.02	0.02	0.20	0.04	0.10	0.12	0.08	0.11	0.05	0.24	0.05	0.05	0.06	0.08
Sr									288.00			185.00	100.00	675.00
F	0.21	0.20	0.15	0.16	0.12	0.12	0.17	0.15	0.07	0.45	0.19	0.08	0.13	0.11
U	45.4	85.2	64.9	29.4	15.3	16.4	194.0	25.1	15.2	42.1	46.9	10.1	12.7	13.8
Th	63.5	23.0	19.0	59.4	48.1	53.3	47.0	69.7	37.2	74.7	57.9	40.6	41.5	42.6

M49A, M408 and M502 majors by rapid rock analysts; J. Reid, analyst. U Th by delayed neutron analysis; H. Millard, M. Coughlin, B. Vaughn, M. Schneider and W. Strang, analysts. M688A,B, M704A,B, and M50 majors by X-ray fluorescence; J.S. Wahlberg, J. Baker, J. Taggert, analysts. FeO, H_2O+, H_2O-, CO_2, F by optical spectroscopy; F. Lichte, H. Neiman, J. Thomas, E. Engleman, G. Mason, and K. King, analysts. M408, M689, M50, INAA; J. Budahn, R. Knight, analysts

Fig. 4 Underground photograph of vertical, flow-banded, brown, glassy dike ("Kerr's dike") cutting fine-grained granite on the Freedom 700 crosscut near the VCA shaft. Dike is about 0.5 m wide and bends to the *right* above the *hammer*. The dike is locally devitrified and contains uranium and molybdenite. Host rock is the Central Intrusion quartz monzonite. The dikes are co-extensive with the uranium deposits and are interpreted to be apophyses on an underlying stock that is genetically related to the deposits. This is the location of sample M408

whole-rock pitchblende + fluorite vein samples. Another age of 16.5 ± 4.3 Ma was obtained using hydrothermal quartz in the veins as a natural external detector for fission tracks from adjacent pitchblende. Sericite from the wallrock adjacent to the Freedom 2A vein on the Freedom 900 level (the deepest available level of the mine) gives a K-Ar age of 20.5 ± 0.7 Ma, which is slightly older, considering that the uranium mineralization postdates the 18.9 ± 0.7 Ma Red Hills Tuff in the Upper and Lower Cloys mines. Here, pitchblende and fluorite ore bodies occur within the tuff and argillically altered rocks extend along the contact with the underlying Central Intrusion.

Structural geology

The main uranium veins in the Central Mining Area occupy near-vertical faults that trend N. 55° to 65°E. (Fig. 3; Kerr et al. 1957; Callaghan 1973). The veins tend to be open space fillings that fill anastomosing structures as much as 0.5 m wide; an example is the Freedom 2A vein on the Freedom 800 level (Fig. 5). Some of the richest ore occurs in steeply plunging shoots at fault intersections. Structures continue at depth but mineralization was non-economic. An important type of vein recognized during underground mapping is flat-lying, commonly concave downward fissure fillings. Where exposed, these veins tend to terminate against near-vertical faults. Where best developed, such as at the west end of the Prospector 200 level in the vicinity of Alvin's stope, the flat-lying veins have a "pull apart", open breccia texture (Fig. 6). It appears that if the matrix material were removed from the vein and the fissure closed, the breccia fragments would fit coherently back together. These flat-lying veins appear to be most

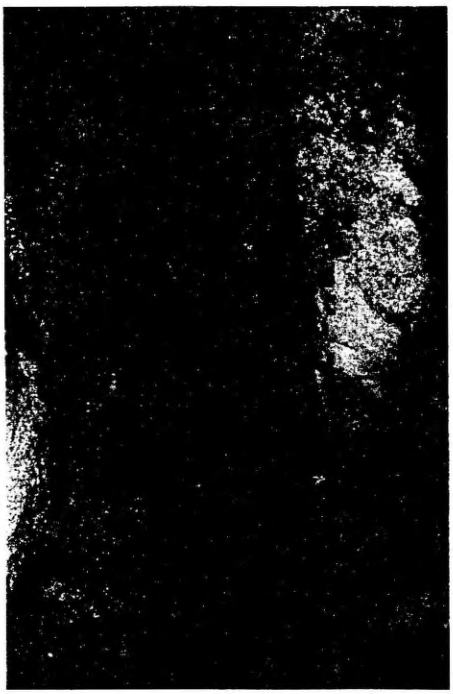

Fig. 5 Vertical exposure of the Freedom 2A vein on the Freedom 800 level showing the anastomosing network of dark veinlets containing fluorite, uraninite, jordisite, coffinite, quartz, and pyrite cutting the lighter colored, sericitized, and pyritized fine-grained granite

Fig. 6 Flat-lying "pull apart" vein on the side of a drift on the Prospector 200 level. Vein material is mostly dark fluorite with uraninite and some pyrite. Light-colored host rock is the Central Intrusion quartz monzonite with local hematite. The "pull apart" motion was vertical and the wall rock fragments can be fit back together if the vein material was removed. *Hammer* is at the *base* of the vein.

abundant in the upper levels of the mines. These veins are somewhat similar in appearance, but not in size, to the near-horizontal veins of the Panasqueira, Portugal, tin-tungsten deposit structures that formed by erosional unloading and hydraulic pressures (Kelly and Rye 1979), but we ascribe a different origin to the Marysvale veins.

Most of the major mines are located in and adjoining blocks that have been uplifted relative to the surrounding area (Fig. 3). The Prospector mine block is an upthrown block bounded by the Prospector 1, 2, and 706 faults (Fig. 3B). Southwest of the Prospector mine, across the Prospector 2 fault, the block is down-dropped and contains the breccia pipe. The wedge-shaped block between the Seegmiller vein and the Bertelsen vein, that includes the Sunnyside shaft and is adjacent to the VCA shaft, is an uplifted block relative to the adjacent blocks. The Freedom 1 vein is down to the north and the Freedom 2A vein is down to the south, indicating that the block between them is uplifted. The three blocks to the north of this, bounded successively on their south sides by the Freedom 1 vein, Freedom 1A vein, and Cloys fault, step down to the north, and the Cloys fault is a reverse fault. The mineralized block containing the Potts shaft and most of the underground workings of the Cloys mine (Fig. 3C) is an anomalous block because it is down-dropped, like a keystone block. The entire highly fractured area of the Central Mining Area thus seems clearly to have been uplifted relative to adjacent less fractured ground, and the areas that were mineralized are generally uplifted the most. Post-mineralization northeast- and northwest-striking basin-range faults cut the uranium veins.

Ore and gangue mineralogy

A description of the mineralogy of the uranium deposits is given in Walker and Osterwald (1956), however, paragenetic information is sparse. Walker and Adams (1963) report early quartz and chalcedony, pyrite, fluorite, and adularia (which could not be confirmed in the present studies) were followed by a period of brecciation, then deposition of these minerals continued along with marcasite, pitchblende, magnetite, hematite, and jordisite; carbonate formed mostly in the late stages along with supergene gypsum and iron and manganese oxides. The principal ore mineral mined at the Central Mining Area was pitchblende that was finely crystalline, granular to massive at depth, and sooty near the surface. Coffinite has been identified from lower levels of the veins. Most pitchblende is intimately associated with jordisite and dark fluorite in anastomosing veinlets; in the deep levels of the mines, banded purple fluorite is in places intergrown with quartz, pitchblende, and coffinite. The fluorite content in most veins increases with depth (Walker and Osterwald 1956), and some fluorite veins are barren of metals. Pyrite content of the ore increases downward, and makes up an estimated 15% of primary vein material in the deepest mine levels (El-Mahady 1966). Pyrite gives way upward, first in a transition zone with hematite vein selvages and above that to more pervasive hematite (Fig. 3B). Molybdenum is widely present in the deposits and in places is as abundant as uranium, although it was not recovered in the treatment process (Kerr 1968; Callaghan 1973). It is present as molybdenite in the glassy dikes. Jordisite (amorphous MoS_2) is the common molybdenum mineral in the veins at depth (Walker and Osterwald 1956), where it can be detected by what the miners called the p-test (jordisite commonly alters to blue ilsemannite ($Mo_3O_8 \cdot nH_2O$) when exposed to urine).

Broken and mineralized ground within 30–40 m of the surface in the Central Mining Area contains a variety of oxidized uranium minerals. These secondary minerals include uranopilite, uranophane, β-uranotile, schroeckingerite, autunite, meta-autunite, johannite, tyuyamunite, rauvite, torbernite, meta-torbernite, phosphuranylite, and zippeite (Walker and Osterwald 1956; Kerr 1968). A new mineral umohoite ($(UO_2)MoO_4 \cdot 4H_2O$) was discovered at Marysvale (Brophy and Kerr 1951) where it has been found chiefly on the 3rd level of the Freedom Number 2 mine. It occurs just below the oxidized zone and may be supergene in origin (Walker and Osterwald 1956). Carbonate, gypsum, and iron and manganese oxides also appear to be mostly secondary minerals. This relationship of supergene uranium minerals to the present surface indicates relatively late oxidation after late Tertiary erosion had exposed the upper parts of the mineralized system. There is no reported enrichment of uranium in the assemblage of secondary minerals overlying the deposit (Walker and Osterwald 1956).

Mineralogical data has been supplemented by chemical analyses to assist characterizing the ore assemblage. Semiquantitative spectrographic analyses of vein samples show that the ore contains as much as 3000 ppm As, 50 ppm Co, 500 ppm Sb, 1500 ppm Tl, trace W, and highly variable Th. Walker and Adams (1963) cite analyses of the ore that indicate the presence of Au, Ag, Cu, Pb, and Y, but they could not be confirmed in analyses as part of this study. X-ray diffraction patterns of mineral separates have shown that minor scheelite is present in the 2A vein at the Freedom 800 level.

Alteration

The uranium veins are surrounded by envelopes of altered rock that flare in width from several cm in the deepest parts of the mines to as much as 2 m at the surface (El Mahady 1966; Kerr 1968). In the deepest accessible level, the Freedom 900 level of the 2A vein, fine-grained granite wallrock is altered to sericite and pyrite in a layer about 5 cm wide on either side of the vein; no hematite is evident. Sample M704A (Table 2) is the sericitized equivalent of sample M704B, the freshest equivalent of which is M50. Sericite replaces feldspar and the mafic minerals are pyritized. X-ray diffraction studies show no kaolinite is present in the wallrock adjacent to the deep veins.

The mineralogy changes systematically upwards. At higher levels, pyrite content in the vein walls decreases, sericite is absent, and the veins are surrounded by a few-cm-wide envelope of hematitized, but much less altered, wallrock. In this hematite transition zone, sample M688A (Table 2), collected adjacent to the vein in the Central Intrusion, is the hematitized equivalent of M688B (collected 5–9 cm from the vein). Sample M688A is characterized by a strong hematite color. Near the present ground surface, above the pyrite-hematite transition zone (Fig. 3B), pyrite is virtually absent, the wallrocks near the veins are altered to kaolinite, sooty pitchblende veins are associated with much more pervasively distributed hematite in the wall rocks, and the widths of vein alteration-mineral envelopes are on the order of a couple of meters. Sample M715 A-F was collected at the ground surface from the Seegmiller vein outwards to 183 cm. Data in Table 2 show that as the vein is approached, hydration, SiO_2, and Al_2O_3 generally increase and FeO, MgO, and CaO decrease.

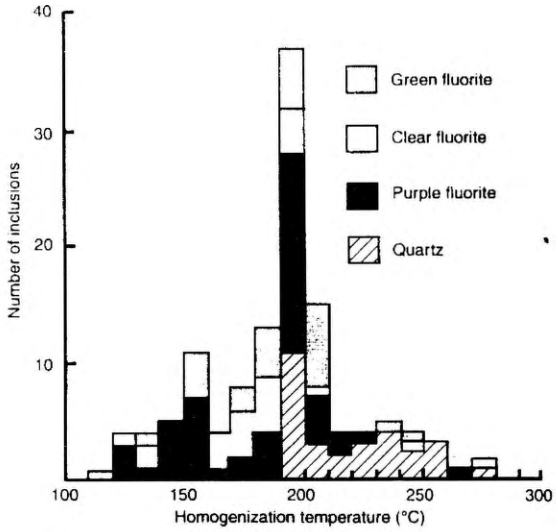

Fig. 7 Histogram of fluid inclusion homogenization temperatures from quartz and fluorite samples from the Central Mining Area, Marysvale, Utah

Fluid inclusions and stable isotopes

Homogenization temperatures and salinities of 132 fluid inclusions were measured in 18 quartz and fluorite samples. The samples and their locations are described in Table 1 and the fluid inclusion data given in Table 3 are plotted on Figs. 7 and 8. Fine-grained quartz is locally intergrown with fluorite. Clear and purple fluorite are commonly part of the same crystal, with clear fluorite having purple growth bands; locally, however, massive purple fluorite occurs without clear fluorite. Green fluorite is generally paragenetically younger than purple fluorite, but in places the sequence is reversed. Vein quartz tends to occur in the deeper levels of the mines, and green fluorite tends to occur at higher levels.

The histogram (Fig. 7) of fluid inclusion homogenization temperatures for all samples shows a peak at about 200 °C. Quartz fluid inclusion temperatures are generally hotter (190–260 °C) than most of the fluorite fluid inclusion temperatures, but there is overlap in the 200–250 °C range. The median homogenization temperatures of fluid inclusions in green and purple fluorite is 190–200 °C, clear fluorite is slightly less at 170–180 °C, and quartz is hotter at 210–220 °C. Coexisting vapor and liquid-rich inclusions in fluorite were found in the near-surface samples and indicate boiling occurred

Table 3 Fluid inclusion data from quartz and fluorite veins in the Central Mining Area, Marysvale, Utah

Sample number	Host mineral	Number of inclusions	Th °C	Salinity wt.% NaCl equivalent	Comments
M29B	clear fluorite	12	135–190	0.18–0.53	Clear fluorite with purple rims
M270	purple fluorite	2	150–151	0	Primary inclusions along purple growth band
M403	euhedral quartz	13	201–271	0.0–0.88	Euhedral quartz crystals that are pre-purple fluorite
M407	purple fluorite	4	189–192	0.18–0.35	Purple fluorite that is younger than green fluorite in same sample
M407	green fluorite	13	196–239	0.18–0.53	Part of sample above
M444	euhedral quartz	13	194–203	0.18–2.24	Euhedral quartz crystals cut by purple fluorite
M547B	quartz	1	230	–	Quartz intergrown with purple fluorite
M663	purple fluorite	11	125–186	0.0–0.53	Purple fluorite vein. Includes homogenization to vapor at 143 °C and 186 °C
M701	purple fluorite	6	121–177	0.88–2.57	Purple fluorite is interbanded with clear fluorite
M701	clear fluorite	5	162–203	0.35–0.88	Part of sample above
M729	quartz	3	230–258	2.07	
M767A	green fluorite	12	130–203	0–0.71	
M767B	purple fluorite	11	192–197	0.71–0.88	Part of sample above
M768	clear fluorite	6	113–272	–	Data highly variable (boiling?)
M768B	purple fluorite	5	188–194	1.4	Part of sample above
M770A	purple fluorite	5	157–262	0.18–1.23	Data highly variable
M770C	clear fluorite	5	120–167	–	Part of sample above
M770D	purple fluorite	6	207–215	1.05–1.23	Part of sample above

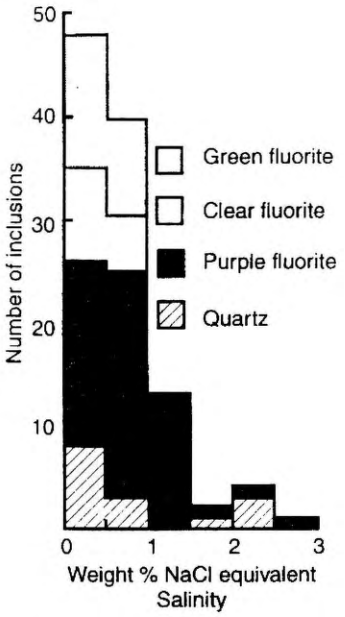

Fig. 8 Histogram of fluid inclusion salinities from quartz and fluorite samples from the Central Mining Area, Marysvale, Utah. Measured freezing point depression temperatures have been modeled on the system NaCl-H_2O and converted to NaCl equivalents (Potter et al. 1978)

at these levels. Fluid inclusion temperatures in minerals deeper in the mine are hotter than those near the present ground surface (Tables 1 and 3). Homogenization temperatures of inclusions in quartz from the Freedom 800 level range from 230–260 °C and most of the inclusions in fluorite from the same level range from 190–220 °C; most homogenization temperatures in both minerals at this level are in the 200–240 °C range. Homogenization temperatures from inclusions in fluorite from the Freedom 1 upper level, high in the mine, are generally in the range of 170–200 °C.

Measured fluid inclusion freezing point depression temperatures were modeled on the system NaCl-H_2O and converted to NaCl equivalents (Potter et al. 1978). The inclusion fluids are generally dilute. The median salinity is 0.0–0.5 wt.% NaCl equivalent for quartz and for green and clear fluorite, and slightly higher, 0.5–1.0 wt.% NaCl equivalent, for purple fluorite. A small, generally rhombic daughter mineral was noted in fluorite of different colors; it did not dissolve upon heating to homogenization temperatures. Carbon dioxide as liquid or clathrates was not found in any samples. In general, the hotter, more saline fluid inclusions are in quartz and the cooler, least saline inclusions are in fluorite.

A series of $\delta^{18}O$ analyses were made on whole rock samples, feldspar separates, and vein quartz to examine the water-rock history of fluids in the veins and wall rock (Table 4). $\delta^{18}O$ values range from 0.2 to 4.0 for whole rock samples and from −3.7 to 6.0 for feldspar phenocryst separates; wallrock samples collected adjacent to the veins vary systematically with depth becoming heavier toward the ground surface (Fig. 9). Two

Table 4 Stable isotope analyses of rock, vein, and mineral samples from the Central Mining Area, Marysvale, Utah

Sample number	$\delta^{18}O$ Whole rock	$\delta^{18}O$ Feldspar	$\delta^{18}O$ Vein quartz	δD Fluid in fluorite	$\delta^{34}S$ Pyrite
M50	1.3	−2.0	–	–	–
M407	–	–	1.5	−133	–
M408	–	–	–	–	−1.5
M547B	–	–	11.4	−137	−4.3
M600	–	–	–	–	4.8
M602	–	–	–	–	−5.0
M621	2.3	4.0	–	–	–
M667	–	–	–	–	−3.8
M674A	3.3	6.0	–	–	–
M688A	1.2	1.2	–	–	–
M688B	3.1	4.0	–	–	–
M699	–	–	–	–	6.2
M702	–	–	–	–	−0.9
M704A	–	−3.7	–	–	0.0
M704B	–	−2.7	–	–	−0.4
M706A	4.0	5.2	–	–	–
M711A	–	−2.4	–	–	−2.9
M715A	4.7	7.4	–	–	–
M715E	4.1	3.9	–	–	–
M715F	3.9	4.5	–	–	–
M729A	0.2	–	–	–	–
M766A	1.3	3.7	–	–	–
M768A	–	–	–	−140	–
M770	–	–	–	−130	–
M776	–	–	–	–	0.9
M777	–	–	–	–	2.7
M793	–	–	–	–	−0.6
M794	–	–	–	–	−1.8
M846	–	–	–	–	6.6

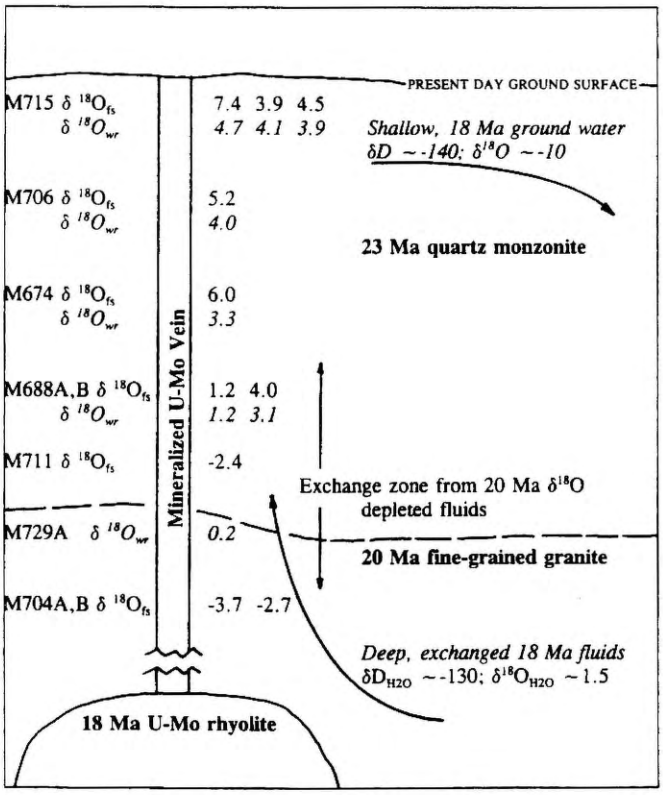

Fig. 9 Diagrammatic cross section through the Central Mining Area showing the relationships between igneous rocks, mineralized rocks, and stable isotope analyses. The $\delta^{18}O$ data from feldspars (subscript *fs*) are shown in *normal print* whereas data from whole rocks (subscript *wr*) are in *italics*. The samples are shown in their relative vertical positions. The values are shown in their relative horizontal positions: the data shown adjacent to the mineralized vein was collected immediately adjacent to the vein and values shown farther to the right were collected successively further away. Detailed sample locations are in Table 1. Relatively fresh 23 Ma quartz monzonite has $\delta^{18}O$ feldspar of 4.0 and whole rock of 2.3. Relatively fresh fine-grained granite (M50) has $\delta^{18}O$ feldspar of −2.0 and whole rock of 1.3

samples of vein quartz gave $\delta^{18}O$ values of 1.5 and 11.4. In addition, δD was examined in inclusion fluids in fluorite and values for four samples range from −140 to −130. These data place constraints on the relative abundance of magmatic and meteoric water components in the hydrothermal fluid. The $\delta^{34}S$ in pyrite have a large range of −5.0 to 6.6 (15 samples, Table 4) and constrain the source of sulfur in the hydrothermal system.

Discussion

Detailed surface and underground geologic mapping, combined with regional relations and geochemical/isotopic fluid inclusion data, provides insight into the genesis of the hydrothermal uranium deposits in the Central Mining Area. Lead and strontium isotopic evidence indicates that the Mount Belknap Volcanics, which are part of the alkali rhyolite end member of the bimodal suite, were derived by partial melting of the batholith that had previously fed the intermediate composition volcanic centers (Cunningham et al. 1994; 1997). Fluorine is 0.07–0.14 wt.% and uranium is 10.1–18.2 ppm in these Mount Belknap volcanic rocks. The Sr content of the glassy dikes associated with the uranium deposits (675 ppm; Table 2) is the highest of any of the alkali rhyolites that were emplaced from 23 to 18 Ma and the silica content (76.76 wt.%, recalculated volatile free) is also the highest in the same rocks. The southwestward progression of igneous activity within the eastern source area probably reflects successive emplacement of shallow stocks above a composite high-level magma chamber (Fig. 2). Peiffert et al. (1996), has shown fractional crystallization in peralkaline suites leads to uranium mineralization. In the Marysvale situation, the changes that took place with time, an increase in silica and volatile content and decrease in phenocryst content, may reflect tapping successively shallower levels of a zoned magma chamber or progressive differentiation of a high-level magma chamber with episodic input of thermal energy.

Structural constraints

Interpretation of the structural evolution of the Central Mining Area is heavily dependent on underground mapping and rock-ore textural observations. Incipient basin-range faulting may have begun with the start of rhyolite volcanism, about 3 Ma before the uranium deposits were formed. The 1:24 000 scale mapping (Cunningham and Steven 1979b; Rowley et al. 1988a) has shown that the area is dominated by largely post-mineralization northeast- and northwest-striking basin-range faults; Osterwald (1965) pointed out that the Central Mining Area is located where these regional faults change direction. Detailed surface and underground mapping has shown that the area corresponding to the Central Mining Area was uplifted relative to the surrounding area (Cunningham and Steven 1979b) prior to this late faulting. The present study demonstrates that the distribution of uranium deposits corresponds to the distribution of individual uplifted blocks.

A structural model is proposed (Fig. 10A–C) to explain the correspondence of the uranium- and molybdenum-bearing rhyolite dikes with the mineralized area and the significance of the breccia pipe and "pull apart" textures in the flat-lying veins. In the model, a rhyolite stock was emplaced into a fractured area, and as magmatic pressure increased, differentially uplifted roof blocks bounded by high-angle faults. Glassy dikes, that are apophyses of the stock, were intruded along the growing faults and these dikes filled faults that offset the contact between the Central Intrusion and fine-grained granite (Fig. 10A). A breccia pipe formed and relieved the upward magmatic pressure (Fig. 10B). As this pressure was relieved, the uplifted blocks began to settle back, but tended to "hang up" so that flat-lying, "pull apart" structures formed by differential downward movement, particularly near high angle faults

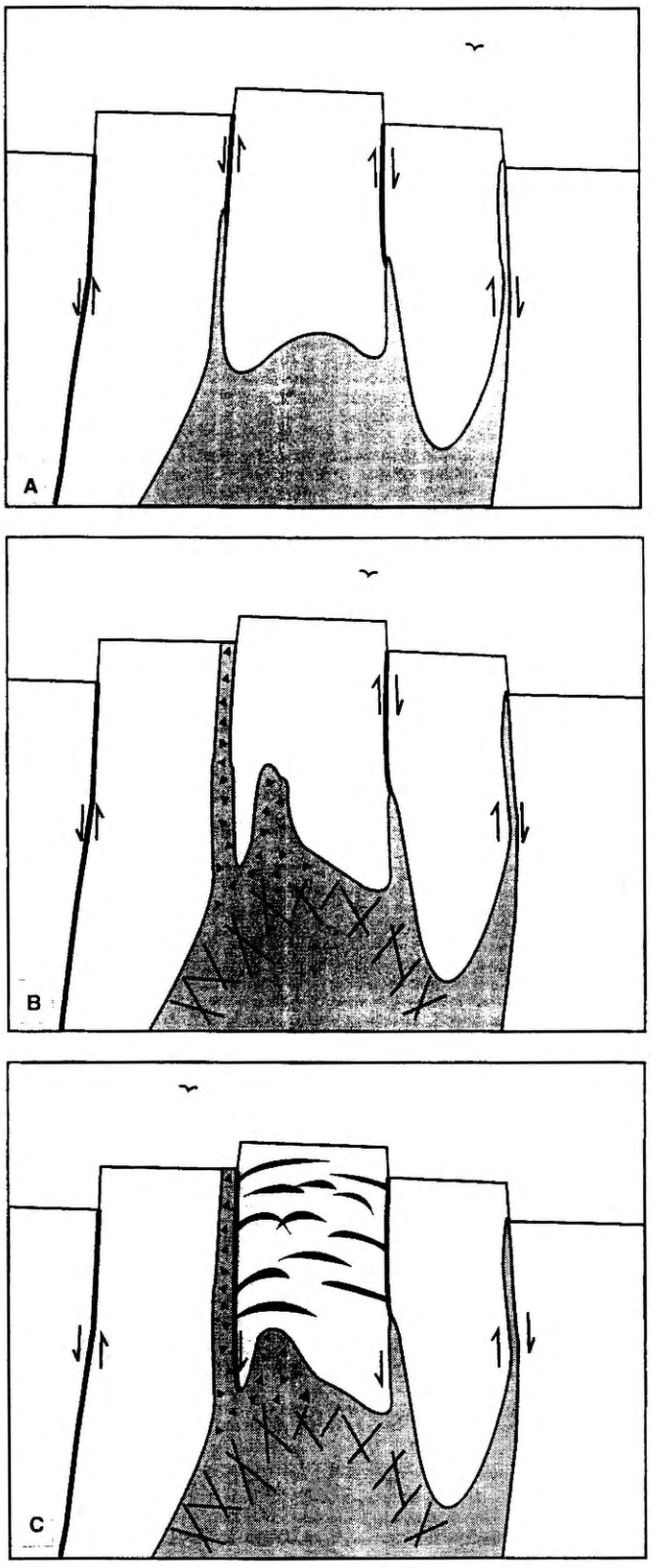

Fig. 10A–C Model for the formation of the uranium deposits of the Central Mining Area, Marysvale, Utah. **A** Intrusion of a rhyolite stock and associated dikes and lifting up of blocks above the stock. **B** Formation of a breccia pipe thus relieving pressure. **C** Blocks return to former position but form flat-lying fractures containing "pull apart" textures that are then mineralized by U-Mo-F fluids associated with the stock. A stockwork molybdenum deposit is postulated to be near the top of the rhyolite stock

(Fig. 10C). Hydrothermal fluids activated by the rhyolite stock permeated the broken carapace and mineralized the high-angle and flat-lying faults.

Fluid inclusion constraints

An estimate of the depth of mineralization comes from fluid inclusion data. The highest temperature at which most fluid inclusions in fluorite from the Freedom 1 upper level homogenize to liquid is about 195 °C; these inclusions contain about 0.8–1.4 wt.% NaCl equivalent, and are associated with sporadic vapor-rich inclusions. These are some of the higher salinities in the deposit and the presence of vapor-rich inclusions suggests sporadic boiling of the fluid as does this slight increase in salinity of the fluids near the surface. The depth beneath the water table at hydrostatic pressures and boiling conditions was about 145 m with a pressure of about 14 bar (Haas 1971) at the Freedom 1 upper level which equates to about 115 m of cover having been eroded from above the present ground surface. Fluid pressures, deduced from fluid inclusion homogenization temperatures in some shallow deposits such as the McLaughlin, California, hot-spring gold deposit, and Julcani, Peru, volcanic dome precious-metal deposit, however, indicate pressures in the upper 200 m of the deposit generally exceeded hydrostatic and episodically exceeded lithostatic (Deen et al. 1994; Sherlock et al. 1995). Modeling the Marysvale data on a lithostatic gradient at 2.7 g/cm^3 gives a depth of about 53 m to the Freedom 1 upper level or about 23 m having been eroded. At these shallow depths, fluid pressures would be expected to be generally hydrostatic and only increase toward lithostatic during episodes of deposition of quartz and fluorite in the vein structures. This depth of 115 m, is reasonable on geologic grounds because the deposit is adjacent to the Red Hills caldera that formed slightly before the deposit and the Red Hills Tuff on the caldera rim would have been piled higher than it is at present.

Mineralogical and thermochemical constraints

The mineralogical associations in the ore, together with thermochemical data, place geochemical constraints on the environment of ore deposition. The vertical zonation of wallrock alteration adjacent to the veins documents the upward changes in the hydrothermal fluid and its interaction with the wallrocks. In the deepest levels of the mine, the sericite-pyrite-fluorite-uraninite-quartz assemblage and lack of hematite suggests that H_2S was the dominant sulfur species, the oxygen fugacity was low, and that the fluids were near neutral. The presence of quartz and coffinite in these deep ores indicates that the hydrothermal system was commonly saturated with silica. Thermochemical constraints suggest the deep fluids had log fO_2 of about −47 to −50 and pH about 6 to 7 (Fig. 11A–C). The general correspondence of fluorite

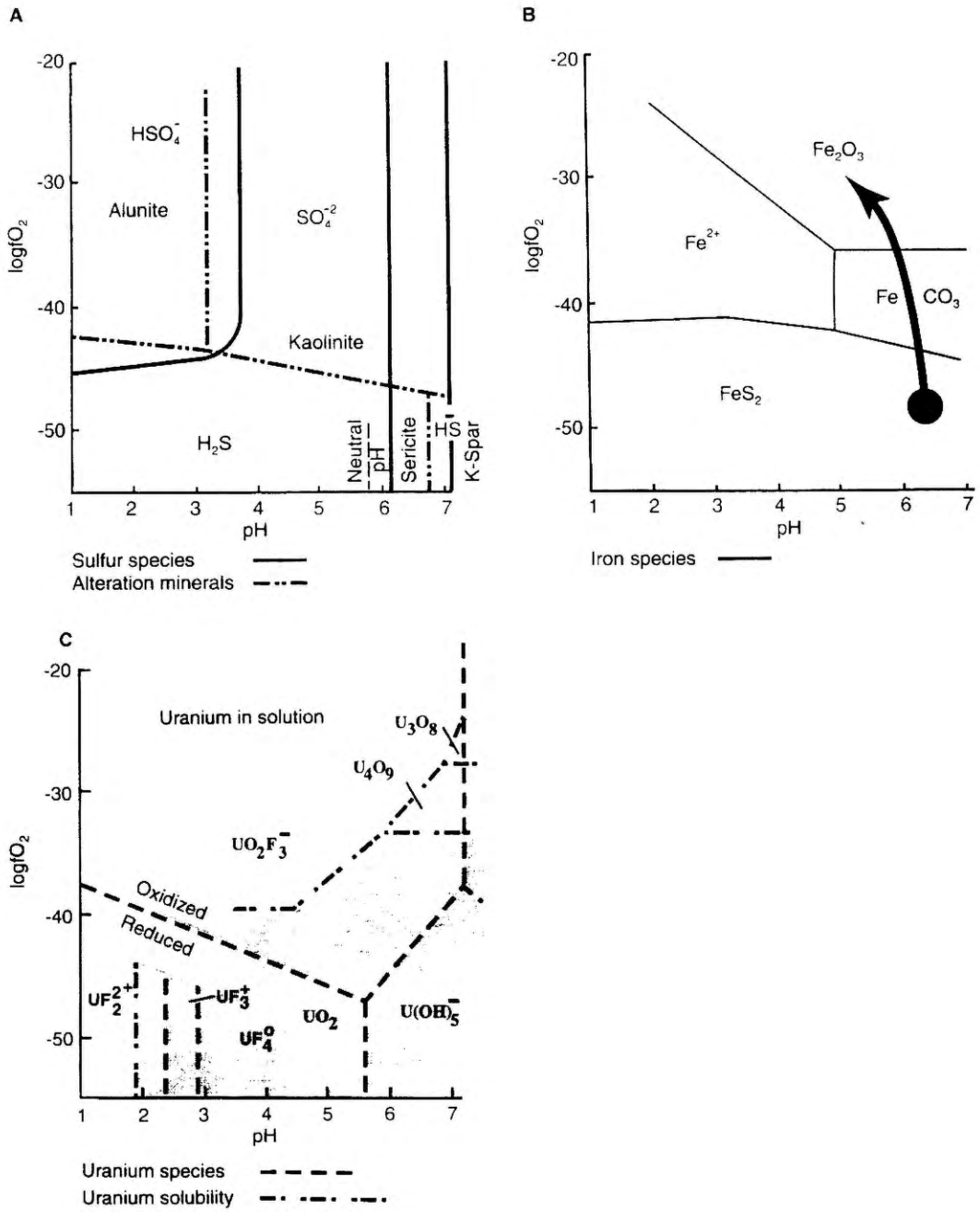

Fig. 11A–C Oxygen fugacity–pH diagram showing the distribution of alteration minerals, sulfur species, uranium species, and uranium solubility in the Central Mining Area uranium deposit. Boundaries are calculated activities. Conditions based on fluid inclusion and mineralogical data are 200 °C, 0.5 m NaCl, 100 ppm F, 100 ppm S, 10 ppm Fe, 100 ppm K, p CO_2 = 1 atm, $\sum U = 0.1$ ppm, quartz present. Coffinite has a stability that is close to that of uraninite + quartz, therefore the uranium solubility for coffinite is closely approximated by the calculations for uraninite. Pyrite is stable in the H_2S field. **A** Sulfur species and alteration minerals; **B** iron species together with *arrow* showing change of conditions as fluids moved to shallower parts of the system; **C** uranium species and solubility with the uraninite field *shaded*

and uraninite in the ore suggests that a uranium-fluorine complex was probably the transporting agent for uranium. Romberger (1984) has shown that fluoride complexes, in particular uranyl trifluoride, are important in the neutral region. Uranous fluoride complexes are important in reducing environments but especially so at lower pHs; hydroxides are stable at neutral pHs (Green and Kerr 1953; Langmuir 1978; Romberger 1984; Parks and Pohl 1988). Sulfidation of the mafics, as observed at the deepest mine levels, can precipitate uranium and free fluorine by the reaction $UO_2F_3^- + FeO$ (in silicates) $+2H_2S = UO_2 + FeS_2 + 3F^- + 2H^+ + H_2O$. Fluorite would be deposited as calcium was released from altered plagioclase, as well as by cooling (Holland and Malinin 1979) of the fluid. The presence of H_2S in the hydrothermal fluid can also act as a reductant for UO_2F_3, releasing F^- to solution. Higher in the system, as sericite plus pyrite in the wall rock gave way to hematite selv-

ages, the formation of hematite and precipitation of uraninite resulted from the coupled redox reaction $UO_2F_3^- + 2FeO$ (in silicates) $+ H_2O = UO_2 + Fe_2O_3 + 3F^- + 2H^+$. At the top of the system, pervasive hematite plus kaolinite and a lack of pyrite are consistent with condensation of volatiles and mixing with shallow, steam-heated waters, resulting in oxidation of H_2S, decrease in pH, and reaction of the fluids with the wall rock (Fig. 11A–C; Barton et al. 1977; Henley 1984; Reed and Spycher 1985).

Isotopic constraints on fluids and minerals

The chemistry of the wallrocks documents the changes in the chemistry of the hydrothermal fluids and the extent that they penetrated into the wallrock adjoining the veins over the vertical range of the mines. The fluid was potassium-rich as shown by the relative increases in K_2O in samples adjacent to the veins (Table 2). At the deepest levels of the mine, the distribution of sericite (sample M704A, Table 2) shows the significantly reactive fluids penetrated about 5 cm from the vein. The elevated K_2O and uranium contents in sample M704B (collected about 10 cm from the vein) shows hydrothermal fluids penetrated at least that far. In the transition zone above, hematitically altered rock adjacent to the vein (sample M688A) contained 194 ppm uranium (Table 2), slightly altered rock about 10 cm from the vein (sample M688B) contained 25 ppm uranium, and unaltered Central Intrusion quartz monzonite (sample M621) contains only 13 ppm uranium. At the ground surface (samples M715 A–F) uranium values significantly above background values have been detected as much as 50 cm into the wall rock (Tables 1 and 2). The elements K, Mo, and W follow a pattern similar to uranium. In contrast, thorium was enriched in vein samples as much as twice, but generally showed little, if any, enrichment in the wall rock. A fission track study of U^{235} distribution adjacent to veins in the Central Intrusion showed nuclide movement by diffusion as much as 5 cm (Shea 1982).

Oxygen isotope studies of the rocks in the Central Mining Area by Shea and Foland (1986) indicate that the rocks underwent massive subsolidus hydrothermal exchange with circulating meteoric water; and our data confirm this and show that much of the exchange was prior to mineralization. The sample of the fine-grained granite (M50) that could be collected furthest away from the mining area has a $\delta^{18}O$ whole rock of 1.3 and a $\delta^{18}O$ of feldspar of −2.0 and the corresponding sample of the quartz monzonite (M621) has a $\delta^{18}O$ whole rock of 2.3 and a $\delta^{18}O$ of feldspar of 4.0 (Table 4). The spatial relation of $\delta^{18}O$ values of wallrock feldspars and whole rocks in a vertical section through the mines is presented schematically in Fig. 9. Samples collected away from the veins and near the fine-grained granite-quartz monzonite contact show low $\delta^{18}O$ values for feldspar that are similar to regional values and probably resulted from isotopic exchange with meteoric waters about 20 Ma, after the fine-grained granite was emplaced. The $\delta^{18}O$ in both feldspar and whole rocks adjacent to the veins becomes systematically heavier upward; whole rock $\delta^{18}O$ changes from 0.2 per mil at depth to 4.7 per mil at the surface and feldspar $\delta^{18}O$ changes from −3.7 per mil at depth to 7.4 per mil at the surface. This, combined with the constraints on depth of penetration of the fluids from the chemical changes, argues for the pattern of isotope signatures in the wall rocks adjacent to the veins being due to interaction with the isotopically heavy water in an 18 Ma hydrothermal fluid. This isotope enrichment in the wallrocks occurs where the hydrothermal alteration typically extends further from the veins. This increased extent of alteration probably coincides with the degassing of acid volatiles from hydrothermal fluids, as suggested by evidence of boiling in the fluid inclusions of shallow samples. This boiling may have resulted in further $\delta^{18}O$ enrichment in the hydrothermal fluids. Also, as shown later from isotopic evidence, this area in the veins was also a mixing zone between the hydrothermal fluids and overlying ground water. Thus, alteration in the wall rocks surrounding the upper part of the veins at Marysvale probably formed in a setting analogous to that in the Creede, CO mining district where the formation of a clay cap resulted from the degassing of hydrothermal fluids and condensation of acid volatiles in the overlying steam-heated ground water (Barton et al. 1977; Bethke 1984).

The δD of the inclusion fluids in the fluorite range from −130 to −140 per mil. The average δD value of magmatic fluids in the Marysvale area was probably close to −70 per mil (e.g., Beaty et al. 1986; and Rye 1993). It is clear that the hydrothermal fluids were dominantly meteoric although they probably contained magmatic components including a small percentage of magmatic water. The $\delta^{18}O_{H_2O}$ of the hydrothermal fluids from the 800 foot level of the Freedom 2A vein in the Freedom mine is about 1.5 per mil as calculated from the $\delta^{18}O$ of quartz and a depositional temperature of 230 °C. This calculated value indicates that the meteoric water hydrothermal fluids were highly exchanged. Such exchanged fluids are consistent with the ^{18}O enriched feldspars and whole rocks in the wall rock alteration in the upper part of the vein systems. The $\delta^{18}O_{H_2O}$ of fluids in equilibrium with vein quartz about 33 m higher in the Sunnyside mine was between −7.9 and −10.9 per mil as calculated from $\delta^{18}O$ values from quartz and from a depositional temperature range of 190 to 240 °C. Vein quartz was obviously deposited in a fluctuating mixing zone between highly exchanged meteoric water hydrothermal fluids and probably steam-heated largely unexchanged ground water much as in the Creede, CO hydrothermal system (Foley et al. 1989; Rye et al. 1988).

The $\delta^{34}S$ values of sulfides range from −5.0 to 6.6 per mil. There is no consistent variation of the $\delta^{34}S$ values in time and space in the veins, and the variations can not easily be assigned to changes in the physical chemical environment of ore deposition. The $\delta^{34}S$ values of drill core in the volcanic rocks underlying the district range

from −15.3 to 5.1 per mil as determined from isotope studies of the alunite deposits in the area (Cunningham et al. 1984). The range of $\delta^{34}S$ values of pyrite in the veins is consistent with an isotopically variable source. The large range of $\delta^{34}S$ values in the sulfur source region may ultimately be due to the fact that prior to volcanism Jurassic evaporite beds originally underlay the district (Cunningham et al. 1984), and repeated magma generation and hydrothermal activity resulted in mixing of the evaporitic sulfate, the products of thermal reduction of the evaporitic sulfate, and magmatic sulfur in magmas and fluids.

Conclusions

The hydrothermal uranium deposits of the Central Mining Area, Marysvale, Utah, were deposited in the fractured roof above a stock from a recurrently active magma chamber during episodic magmatic evolution of that chamber. The stock lifted overlying rocks as fault blocks and led to formation of a breccia pipe; escape of magma and volatiles from the breccia pipe relieved magmatic pressure, and as the blocks settled back, flat-lying fractures with "pull apart" textures formed locally. The source stock was intruded into a cluster of older stocks that shielded the fluids from interaction with the sedimentary rocks that underlie the volcanic field and are exposed on Deer Trail Mountain.

The wallrocks were altered by low ^{18}O meteoric water fluids prior to mineralization and probably right after the intrusion of the 20 Ma granite. Mineralization in the Central Mining Area was related to intrusion of the 18 Ma stock. Geologic reconstruction and fluid inclusion and stable isotope data support a near surface (23–115 m) depth of formation of the deposit near the fluctuating interface between an exchanged meteoric water and overlying steam-heated ground water. Episodes of ore deposition from the hydrothermal fluids were probably rapid, as suggested by the triggering action of a breccia pipe, the presence of jordisite (amorphous MoS_2), and the generally fine-grained nature of the ore. Isotopically exchanged, U-Mo-F-H_2S bearing, meteoric water hydrothermal solutions with at least 3% salinity entered the fractures at depth at about 240 ± 20 °C and deposited a uraninite-fluorite-pyrite-coffinite-quartz mineral assemblage in the veins and altered the wallrocks to sericite. The temperature varied from about 240 °C to 190 °C over the 300 m vertical interval of the exposed mine workings. These fluids boiled and the degassed volatiles probably condensed in overlying steam-heated ground water. The resulting changes in oxidation state and pH of these fluids led to the hematite selvages and kaolinitized wall rocks in the upper part of the ore bodies. Uranium is interpreted to have been transported mostly as uranyl trifluoride complexes and deposited as fluids reacted with the wallrocks and mixed with steam-heated ground water. Supergene alteration in the area led to the formation of secondary minerals and probably gypsum and some of the shallow hematite alteration.

Acknowledgements The authors thank Steve Ransom for his assistance with computer drafting, Energy Fuels Corporation for allowing access to the mines and allowing and supporting JDR's participation in the study. We appreciate thought-provoking and helpful reviews by Paul Barton, Philip Goodell, Richard Grauch, Jean Dubessy, B.A. Hofmann, and Bill Miller.

References

Anderson JJ, Rowley PD (1975) Cenozoic stratigraphy of southwestern High Plateaus of Utah. In: Anderson JJ, Rowley PD, Fleck RJ, Nairn AEM (eds) Cenozoic geology of southwestern High Plateaus of Utah. Geol Soc Am Spec Pap 160: pp 1–51

Barton PB Jr, Bethke PB, Roedder E (1977) Environment of ore deposition in the Creede mining district, San Juan mountains, Colorado: Part III. Progress toward interpretation of the chemistry of the ore-forming fluid for the OH vein. Econ Geol 72: 1–24

Beaty DW, Cunningham CG, Rye RO, Steven TA, Gonzalez-Urien E (1986) Geology and geochemistry of the Deer Trail Pb-Zn-Ag-Au-Cu manto deposits, Marysvale district, west-central Utah. Econ Geol 81: 1932–1952

Best MG, McKee EH, Damon PE (1980) Space-time-composition patterns of late Cenozoic mafic volcanism, southwestern Utah and adjoining areas. Am J Sci 280: 1035–1050

Bethke PM (1984) Controls on base- and precious-metal mineralization in deeper epithermal environments. US Geol Surv Open-File Rep 84-890: 40

Brophy GP, Kerr PF (1951) Hydrous uranium molybdate in Marysvale ore. Ann Rep June 30, 1952 to April 1, 1953, US Atomic Energy Comm, RME-3046: 45–51

Bromfield CS, Grauch RI, Otton JK, Osmonson LM (1982) National Uranium Resource Evaluation of the Richfield quadrangle, Utah. US Department of Energy Rep PGJ/F-044(82): 94 p, 13 plts

Budding KE, Cunningham CG, Zielinski RA, Steven TA, Stern CR (1987) Petrology and chemistry of the Joe Lott Tuff member of the Mount Belknap Volcanics, Marysvale volcanic field, west-central Utah. US Geol Surv Prof Pap 1354: 47 p

Callaghan E (1939) Volcanic sequence in the Marysvale region in southwest-central Utah. Trans Am Geophys Union 20(3): 438–452

Callaghan E (1973) Mineral resource potential of Piute County, Utah and adjoining area. Utah Geol Min Surv Bull 102: 135 p

Callaghan E, Parker RL (1961) Geology of the Monroe Quadrangle, Utah. US Geol Surv Geol Quad Map GQ-155. Scale 1:24,000

Cunningham CG, Steven TA (1979a) Mount Belknap and Red Hills calderas and associated rocks, Marysvale volcanic field, west-central Utah. US Geol Surv Bull 1468: 34

Cunningham CG, Steven TA (1979b) Uranium in the Central Mining Area, Marysvale District, west-central Utah. US Geol Surv Misc Invest Series Map I-1177

Cunningham CG, Steven TA (1979c) Geologic map of the Deer Trail Mountain-Alunite Ridge mining area, west-central Utah. US Geol Surv Misc Invest Series Map I-1230

Cunningham CG, Steven TA, Rasmussen JD (1980) Volcanogenic uranium deposits associated with the Mount Belknap volcanics, Marysvale volcanic field, west-central Utah (Abstr). Energy exploration in the 80's, Annual meeting of the southwest section, Am Assoc Petrol Geol El Paso, Texas, Feb. 25–27, 1980, p 22

Cunningham CG, Ludwig KR, Naeser CW, Weiland EK, Mehnert HH, Steven TA, Rasmussen JD (1982) Geochronology of hydrothermal uranium deposits and associated igneous rocks in the eastern source area of the Mount Belknap volcanics, Marysvale, Utah. Econ Geol 77: 453–463

Cunningham CG, Rye RO, Steven TA, Mehnert HH (1984) Origins and exploration significance of replacement and vein-type alunite deposits in the Marysvale volcanic field, west central Utah. Econ Geol 79: 50–71

Cunningham CG, Steven TA, Rowley PD, Naeser CW, Mehnert HH, Hedge CE, Ludwig KR (1994) Evolution of volcanic rocks and associated ore deposits in the Marysvale volcanic field, Utah. Econ Geol 89: 2003–2005

Cunningham CG, Rye RO, Bethke PM, Logan MAV (1996) Formation of coarse-grained vein alunite by degassing of an epizonal stock (Abstr). Proc Chapman Conf on crater lakes, terrestrial degassing and hyper-acid fluids in the environment, 5–9 September, 1996, Crater Lake, Oregon, 27

Cunningham CG, Unruh DM, Steven TA, Rowley PD, Naeser CW, Mehnert HH, Hedge CE, Ludwig KR (1997) Geochemistry of volcanic rocks in the Marysvale volcanic field, west-central Utah. In: Friedman J D, Huffman A C (eds) Laccolith complexes of southeastern Utah–Tectonic control and time of emplacement. US Geol Surv Bull (in press)

Curtis L (1981) Uranium in volcanic and volcaniclastic rocks-examples from Canada, Australia, and Italy. In: Goodell PC, Waters AC (eds) Uranium in volcanic and volcaniclastic rocks. Am Assoc Petrol Geol Studies in Geology 13: pp 37–53

Deen JA, Rye RO, Munoz JL, Drexler JW (1994) The magmatic hydrothermal system at Julcani, Peru: evidence from fluid inclusions and hydrogen and oxygen isotopes. Econ Geol 89: 1924–1938

Dunkhase JA (1980) A comparative study of the whole rock geochemistry of the uranium mineralized Central Intrusive at Marysvale, Utah to nonmineralized intrusives in southwest Utah. Unpub PhD dissertation Colorado School of Mines, Golden, 130 p

El-Mahady OR (1966) Origin of ore and alteration in the Freedom No. 2 and adjacent mines at Marysvale, Utah. Unpub PhD dissertation University of Utah, Salt Lake City, 217 p

Foley NK, Bethke PM, Rye RO (1989) A reinterpretation of the $\delta^{18}O_{H_2O}$ of inclusion fluids in contemporaneous quartz and sphalerite, Creede mining district, Colorado: a generic problem for shallow ore bodies? Econ Geol 84: 1966–1977

George-Aniel B, Leroy J, Poty B (1985) Uranium deposits of the Sierra Peña Blanca: Three examples of mechanisms of ore deposit formation in a volcanic environment. In: Uranium deposits in volcanic rocks, Proc Technical Committee Meeting, El Paso, Texas, 2–5 April 1984. International Atomic Energy Agency, Vienna, pp 175–186

Gilbert RE (1957) Notes on the relationship of uranium mineralization and rhyolite in the Marysvale area, Utah. US Atomic Energy Comm Rpt RME-2030: 29 p

Goddard EN (1935) The influence of Tertiary intrusive structural features on mineral deposits at Jamestown, Colorado. Econ Geol 30: 370–386

Goddard EN (1946) Fluorspar deposits of the Jamestown district, Boulder County, Colorado. Colorado Sci Soc Proc 15(1): 47 p

Goodell PC (1985) Chihuahua City uranium province, Chihuahua, Mexico. In: Uranium deposits in volcanic rocks, Proc Technical Committee Meeting, El Paso, Texas, 2–5 April 1984. International Atomic Energy Agency, Vienna, 97–124

Goodell PC, Waters AC (eds) (1981) Uranium in volcanic and volcaniclastic rocks. Am Assoc Petrol Geol Studies in Geology 13, 331 p

Green J, Kerr PF (1953) Geochemical aspects of alteration, Marysvale, Utah. Atomic Energy Comm Ann Rep June 30, 1952–April 1, 1953, RME-3046: 73–99

Gruner JW, Fetzer WG, Rapaport I (1951) The uranium deposits near Marysvale, Piute County, Utah. Econ Geol 46: 243–251

Haas JL Jr (1971) The effect of salinity on the maximum thermal gradient of a hydrothermal system at hydrostatic pressure. Econ Geol 66: 940–946

Henley RW (1984) Gaseous components in geothermal systems. Reviews in Econ Geol 1: 45–56

Holland HD, Malinin SD (1979) The solubility and occurrence of non-ore minerals. Chapt 9. In: Barnes HL (ed) Geochemistry of hydrothermal ore deposits. John Wiley and Sons, New York, pp 461–508

International Atomic Energy Agency (1985) Uranium deposits in volcanic rocks. IAEA-TC-490/19. Proc Tech Comm Mtg, El Paso, Texas, 2–5 April 1984. International Atomic Energy Agency, Vienna, 468 p

Kelly WC, Goddard EN (1969) Telluride ores of Boulder County, Colorado. Geol Soc Am Mem 109: 237 p

Kelly WC, Rye RO (1979) Geologic, fluid inclusion, and stable isotope studies of the tin-tungsten deposits of Panasqueira, Portugal. Econ Geol 74: 1721–1822

Kerr PF (1968) The Marysvale, Utah, uranium deposits. In: Ridge JD (ed) Ore deposits of the United States, 1933–1967 (Graton-Sales vol) vol 2: New York, American Institute of Mining Metallurgy Petroleum Engineers, pp 1020–1042

Kerr PF, Brophy GP, Dahl HM, Green J, Woolard LE (1957) Marysvale, Utah, uranium area. Geol Soc Am Spec Pap 64: 212 p

Langmuir D (1978) Uranium solution-mineral equilibria at low temperatures with applications to sedimentary ore deposits. Geochim Cosmochim Acta 42: 547–570

Lindsey DA (1981) Volcanism and uranium mineralization at Spor Mountain, Utah. In: Goodell PC, Waters AC (eds) Uranium in volcanic and volcaniclastic rocks. Am Assoc Petrol Geol Studies in Geology 13: 89–98

Morton RD, Aubut A, Ghandi SS (1978) Fluid inclusion studies and genesis of the Rexpar uranium-fluorite deposit, Birch Island, British Columbia. In: Current Research, Part B, Canadian Geol Surv Pap 78–1B: pp 137–140

Nash JT, Cunningham CG (1973) Fluid inclusion studies of the fluorspar and gold deposits, Jamestown district, Colorado. Econ Geol 68: 1247–1262

O'Rourke PJ (1975) Maureen uranium-fluorine-molybdenum prospect, Georgetown. In: Knight CL (ed) Economic geology of Australia and Papua New Guinea: Aust Inst Mining Metal, Monogr 5: 764–769

Osterwald FW (1965) Structural control of uranium-bearing vein deposits and districts in the conterminous United States. US Geol Surv Prof Pap 455-G: 23 p

Parks GA, Pohl DC (1988) Hydrothermal solubility of uraninite. Geochim Cosmochim Acta 52: 863–875

Peiffert C, Nguyen-Trung C, Cuney M (1996) Uranium in granitic magmas: part 2. Experimental determination of uranium solubility and fluid-melt partition coefficients in the uranium oxide-haplogranite-H_2O-NaX (X = Cl, F) system at 770 °C, 2 kbar. Geochim Cosmochim Acta 60: 1515–1529

Phair G, Shimamoto KO (1952) Hydrothermal uranothorite breccias from the Blue Jay mine, Jamestown, Boulder County, Colorado. Am Min 37: 659–666

Potter RW II, Clynne MA, Brown DL (1978) Freezing point depression of aqueous sodium chloride solutions. Econ Geol 73: 284–285

Preto VA (1978) Setting and genesis of uranium mineralization at Rexpar. Can Inst Mining Metal Bull 70: 93–100

Rasmussen JD, Cunningham CG, Steven TA, Rye RO, Romberger SB (1985) Origin of hydrothermal uranium vein deposits in the Marysvale volcanic field (Abstr). In: Uranium deposits in volcanic rocks Proc Technical Committee Meeting, El Paso, Texas, April 2–5, 1984, International Atomic Energy Agency, Vienna, Austria, 317

Reed MH, Spycher NF (1985) Boiling, cooling and oxidation in epithermal systems: a numerical modeling approach. Rev Econ Geol 2: 249–272

Rich RA, Holland HD, Petersen U (1977) Hydrothermal uranium deposits. Developments in Econ Geol 6, Elsevier, New York: 264 p

Romberger SB (1984) Transport and deposition of uranium in hydrothermal systems at temperatures up to 300 °C: geological implications. In: De Vivo B, Ippolito F, Capaldi G, Simpson PR (eds) Uranium geochemistry, mineralogy, geology, exploration and resources: The Institute of Mining and Metallurgy, London, England, 12–18

Rowley PD, Cunningham CG, Steven TA, Mehnert HH, Naeser CW (1988a) Geologic map of the Marysvale quadrangle, Piute County, Utah. Utah Geol Min Survey Map 105

Rowley PD, Cunningham CG, Steven TA, Mehnert HH, Naeser CW (1988b) Geologic map of the Antelope Range quadrangle, Sevier and Piute Counties, Utah. Utah Geol Min Survey Map 106

Rowley PD, Mehnert HH, Naeser CW, Snee LW, Cunningham CG, Steven TA, Anderson JJ, Sable EG, Anderson RE (1994) Isotopic ages and stratigraphy of Cenozoic rocks of the Marysvale volcanic field and adjacent areas, west-central Utah. US Geol Surv Bull 2071: 35 p

Rye RO (1993) The evolution of magmatic fluids in the epithermal environment: the stable isotope perspective. Econ Geol 88: 733–753

Rye RO, Plumlee GS, Bethke PM, Barton PB Jr (1988) Stable isotope geochemistry of the Creede, Colorado, hydrothermal system US Geol Surv Open-File Rpt 88-356: 38 p

Shea ME (1982) Uranium migration associated with some hydrothermal veins at Marysvale, Utah: a natural analog for radioactive waste isolation. Unpub MS Thesis, Univ Calif Riverside: 123 p

Shea M, Foland KA (1986) The Marysvale natural analog study: preliminary oxygen isotope relations. Chem Geol 55: 281–295

Sherlock RL, Tosdal RM, Lehrman NJ, Graney JR, Losh S, Jowett EC, Kesler SE (1995) Origin of the McLaughlin mine sheeted vein complex: metal zoning, fluid inclusion, and isotopic evidence. Econ Geol 90: 2156–2181

Staatz MH, Osterwald FW (1956) Uranium in the fluorspar deposits of the Thomas Range, Utah. In: Page LR, Stocking HE, Smith HB (Compilers) Contributions to the geology of uranium and thorium by the US Geol Surv and Atomic Energy Commission for the United Nations Int Conf on Peaceful Uses of Atomic Energy, Geneva, Switzerland, 1955: US Geol Surv Prof Pap 300: pp 131–136

Staatz MH, Osterwald FW (1959) Geology of the Thomas Range fluorite district, Juab County, Utah. US Geol Surv Bull 1069: 97 p

Steven TA, Morris HT (1987) Summary mineral resource appraisal of the Richfield 1° × 2° quadrangle, west-central Utah. US Geol Surv Circ 916: 24 p

Steven TA, Cunningham CG, Naeser CW, Menhert HH (1979) Revised stratigraphy and radiometric ages of volcanic rocks in the Marysvale area, west-central Utah. US Geol Surv Bull 1469: 40 p

Steven TA, Cunningham CG, Machette MN (1981) Integrated uranium systems in the Marysvale volcanic field, west-central Utah. In: Goodell PC, Waters AC (eds) Uranium in volcanic and volcaniclastic rocks. Am Assoc Petrol Geol Studies in Geology 13: 111–122

Steven TA, Rowley PD, Cunningham CG (1984) Calderas of the Marysvale volcanic field, west central Utah. J Geophys Res 89 (B10): 8751–8764

Taylor AO, Anderson TP, O'Toole WL, Waddell GG, Gray AW, Douglas H, Cherry CL, Caywood RM (1951) Geology and uranium deposits of Marysvale, Utah. Interm report on the producing area, US Atomic Energy Comm RMO-896: 30 p

US Geological Survey (1963) Geology of uranium-bearing veins in the conterminous United States. US Geol Surv Prof Pap 455: 146 p

Walker GW, Adams JW (1963) Mineralogy, internal structural and textural characteristics, and paragenesis of uranium-bearing veins in the conterminous United States. US Geol Surv Prof Pap 455-D: 35 p

Walker GW, Osterwald FW (1956) Relation of secondary uranium minerals to pitchblende-bearing veins at Marysvale, Piute County, Utah. In: Page LR, Stocking HE, Smith HB (eds) Contributions to the geology of uranium and thorium by the United States Geological Survey and Atomic Energy Commission for the United Nations international conference on the peaceful uses of atomic energy, Geneva, Switzerland 1955. US Geol Surv Prof Pap 300: 123–129

Walker GW, Osterwald FW (1963) Introduction to the geology of uranium-bearing veins in the conterminous United States: US Geol Surv Prof Pap 455-A: 28 p

Willard ME, Callaghan E (1962) Geology of the Marysvale Quadrangle, Utah. US Geol Surv Geol Quad Map GQ-154, Scale 1:24,000

International Journal for Geology, Mineralogy and Geochemistry of Mineral Deposits

Official Bulletin of the Society for Geology Applied to Mineral Deposits

Volume 33 Number 5 1998

Online edition in LINK
Geosciences Online Library
http://link.springer.de

Indexed in *Current Contents*
33 (5) 437–538 June 1998
Printed on acid-free paper

Springer

0026-4598(199807)33:5;1-R